Journal of Materials and Environmental Science
ISSN : 2028-2508
e-ISSN : 2737-890X
CODEN : JMESCN

J. Mater. Environ. Sci., 2024, Volume 15, Issue 9, Page 1307-1320

http://www.jmaterenvironsci.com

Elaboration and characterization of clay nanoparticles for Cr (VI) elimination in water

Goro H. H. [1], Sorgho B. [1*], Ouedraogo R. D. [1], Bakouan C. [1], Guel B. [1], Blanchart P. [2]

[1] *Laboratory of Molecular Chemistry and Materials, University Joseph KI-ZERBO, 03 BP 7021 Ouaga 03, Burkina Faso*
[2] *University of Limoges, CNRS, IRCER, UMR 7315, F-87000 Limoges, France*

**Corresponding author, Email address: sorghobrahima3@gmail.com*

Received *28 Aug 2024,*
Revised *23 Sept 2024,*
Accepted *24 Sept 2024*

Citation*: Goro H. H., Sorgho B., Ouedraogo R. D., Bakouan C., Guel B., Blanchart P. (2024) Elaboration and characterization of clay nanoparticles for Cr (VI) elimination in water, J. Mater. Environ. Sci., 15(9), 1307-1320*

Abstract: Environmental chromium pollution in Burkina Faso is increasing in relation to industrial development. This growth of this heavy metal in water leads to the need to find accessible and effective adsorbents to ensure their elimination. Thus, we were interested in new generations of adsorbents, Kaolinite Nanoparticles (KNP) which were obtained from a local clay, rich in kaolinite, called KOU. The use of KNP for Cr(VI) removal showed that equilibrium was reached after 3 hours of contact time and that adsorption follows a pseudo-second order kinetic model. This suggests the existence of chemisorption. Dose effect results showed removal up to 90% and maximum chromium (VI) adsorption was observed at pH=2. Modeling of the experimental data showed that the adsorption isotherms are more in agreement with the Langmuir model.

Keywords: *chromium; elimination; Kaolinite Nanoparticles (KNP); Chemisorption*

1. Introduction

Environmental protection has become a major economic and political issue in view of the increasingly growing threats of pollution due to heavy metals. A large portion of these metals comes from metal salts which are widely used in many industrial processes such as electroplating, textile, tanneries, dyeing, metal finishing industries, etc. (Alasadi *et al.*, 2019). Tannery industries use of chemical reagents which mostly produce toxic heavy metals (Prasad *et al.*, 2021). Heavy metals are metallic elements with a density greater than 5 g.cm^{-3} (Bazié *et al.*, 2022), which are non-biodegradable and accumulate easily in living organisms through the food chain (Zhang *et al.*, 2019). They are relatively abundant in the earth's crust and are often used in industrial processes and agriculture. Heavy metals are transported by run-off water and contaminate water sources downstream of the industrial site. Lead (Pb), arsenic (As), cadmium (Cd), mercury (Hg), chromium (Cr), zinc (Zn), nickel (Ni) and copper (Cu) are common metals found in wastewater (Tariq, 2021; Errich *et al.*, 2021; Azzaoui *et al.*, 2019; Razzouki *et al.*, 2015; El Harti *et al.*, 2013). Some of these heavy metals (Zn and Cu) play a vital role in human metabolism at low concentrations, but can become toxic when their concentration

exceeds the recommended level. However, heavy metals such as lead, mercury and cadmium are harmful to living organisms, even in low concentrations, and still play no particular role in metabolism (Tariq, 2021). All living micro-organisms, plants and animals depend on water for their survival, and as heavy metals can bind to the surface of micro-organisms, they can be transported within the cell. In fact, heavy metals can be chemically transformed by chemical reactions similar to those involved in the digestion of food (Prasad *et al.*, 2021). The release of heavy metals into the aquatic environment can cause major disturbances. Plants in aquatic systems react to these disturbances by decreasing their density, diversity and species composition (Vardhan *et al.*, 2019). According to Njuguna *et al.*, (2019), heavy metals such as Cd, Cu and Pb are responsible for gastrointestinal cancer, which accounts for around 25% of all fatal cancers worldwide. Chromium exists in the environment in two main oxidation states, trivalent chromium (Cr(III)) and hexavalent chromium (Cr(VI)) (Prasad *et al.*, 2021). However, Cr(III) is an essential element for living organisms at low concentrations (Prasad *et al.*, 2021) and for the maintenance of several metabolic pathways. The toxicity of Cr(III) is relatively low due to the slowness of its ligand exchange kinetics, which makes it relatively unreactive. Cr(VI) is one of the heavy metals that has received special attention in wastewater treatment, Cr(VI) is toxic even at parts per billion levels (Pakade *et al.*, 2019). Prasad *et al.*, (2021) reported that Cr(VI) contamination of drinking water, soil and crops due to high levels of exposure to Cr(VI)-polluted wastewater was widely associated with a 60-fold increase in stomach cancer rates.. According to the United States Environmental Protection Agency, the maximum concentration of Cr(VI) allowed in drinking water is 0.01 mg/L and less than 0.05 mg/L in surface water (Ukhurebor *et al.*, 2021). In Burkina Faso, environmental chromium pollution is a challenge given the growing industrialization of recent years (Sawadogo & Zoungrana, 2024).

The penetration and bio-accumulative power of heavy metals in food chains and their toxicity to biological systems as a result of increasing concentrations over time have led to considerable pressure for their separation and purification. Several remediation methods have been developed to reduce the risks. Conventional processes for removing heavy metals from wastewater include chemical precipitation, flotation, adsorption, ion exchange and electrochemical deposition. The limitations of many of these treatment methods are the production of secondary waste and the high cost of operation and maintenance (Vardhan *et al.*, 2019). Adsorption is a process of separation through which adsorbate is transferred from the liquid phase to the surface of the absorbent and becomes bound by physical and chemical interactions (Ukhurebor *et al.*, 2021). The use of clays as adsorbents offers advantages over many other commercially available adsorbents in terms of low cost, availability, high specific surface area and greater potential for ion exchange conducive to adsorption processes.

Nanotechnology has contributed to the development of new products and alternative processes for water purification. This involves reducing the size of the particles, thereby increasing their specific surface area. Nano-technology could be the best strategies for the eco-friendly restoration of Chromium contaminated sites (Prasad *et al.*, 2021).

To deal with this growing pollution, we propose to use new generations of adsorbents, Nano-Kaolinites which are little studied in Burkina. They will be produced from natural clays using an ecological synthesis method using non-toxic, less expensive and non-polluting solvents (Alasadi *et al.*, 2019). The Nano-Kaolinites will be characterized using several techniques before being used for the elimination of Cr(VI) depending on the dose of adsorbent, the pH of the solution, the kinetics of absorption as well as the concentration of Cr(VI).

2. Methodology

2.1 Sourcing and preparation of clay nanoparticles

A natural clay called KOU (**Figure 1**) was used as a precursor for kaolinite nanoparticles. It was taken in the rural municipality of Komsilga, located at 25 km south of Ouagadougou, the capital of Burkina Faso.

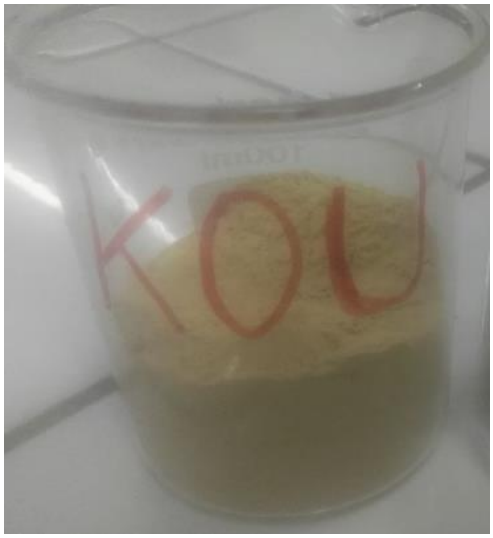

Figure 1. KOU sample

2.2 Experiments

2.2.1. Synthesis of clay nanoparticles

The synthesis method was carried out following the acid extraction method (Alasadi *et al.*, 2019). The clay was crushed then sieved with a 160 µm sieve. The sieve bottom obtained was dried in an oven at 80°C for 4 hours. Then, in a 250 mL Erlenmeyer flask, 50 g of the dried KOU powder were dispersed in 200 mL of a 37% HCl solution, then the whole was stirred at 460 rpm at room temperature for 6 hours. After decantation, the product obtained was filtered then washed with distilled water until almost all of the chloride ions were eliminated. The final solid residue was dried in an oven and then ground to obtain a white clay powder (**Figure 2**) called kaolinite nanoparticles (KNP***)***.

2.2.2. Application of nano kaolinite for elimination of chromium (VI)

A stock solution of Cr(VI) with a concentration of 50 mg/L was prepared from a potassium dichromate salt, K_2CrO_4. For each test, an appropriate mass of KNP was introduced into 100 mL Erlenmeyer flask containing 50 mL of Cr(VI) solution. The mixture obtained was stirred for the allotted time then filtered using a 25 mm diameter nylon membrane with a retention threshold of 0.45 µm. The residual Cr(VI) concentration is measured by flame atomic absorption spectrometry (SAAF).

Parameters that can affect Cr(VI) adsorption by KNP such as contact time, pH, adsorbent dose and initial Cr(VI) concentration were investigated. The initial pH of the solutions was adjusted with a solution of hydrochloric acid (HCl) with a concentration of 0.1 mol/L and sodium hydroxide (NaOH) with a concentration of 0.1 mol/L. To study the kinetics, 0.01 g of KNP was introduced into Cr(VI) solution with a concentration of 0.02 mg/L. The pH of the initial solutions was adjusted to 2 then the mixtures were stirred at 300 rpm between 30-240 min. To determine the pH effect, solutions of Cr(VI) with a concentration of 0.02 g/L as well as 0.1 g of KNP were introduced into the different solutions

then the whole was stirred at 300 rpm for 180 min. Increasing concentrations of KNP ranging from 0 to 2 g were used to examine the dose effect. For these tests, Cr(VI) solutions with a concentration of 0.02 g/L were used and the pH was adjusted to 2 then stirred at 300 rpm for 180 min. The concentration effect was carried out on Cr(VI) solutions with concentrations ranging from 0 to 0.025 g/L. In each solution, 0.1 g of KNP was added and the pH adjusted to 2 then the whole was stirred for 180 min.

Figure 2. KNP sample

2.3 Characterization of raw materials and products

Raw materials (KOU) and products (KNP) used in the process were characterized using inductively coupled plasma-optical emission spectrometry (ICP-OES), X-ray diffraction (XRD) X, Fourier Transform Infra-Red Spectroscopy (FTIR) and Brunauer-Emmet-Teller (BET) analysis.

3. Results and Discussion

3.1. Characterization of KOU

The elemental chemical analysis of KOU (**Table 1**) shows the predominance of silica and alumina in the sample. This is characteristic of clays containing kaolinite and quartz. The mass ratio of $(SiO_2)/(Al_2O_3)$ = 2.06 is relatively higher than that of pure kaolins which is 1.18. This difference indicates the presence of free Quartz in the clay (Kieufack *et al.*, 2023). The relatively high content of Fe_2O_3 would be responsible for the color of KOU. We also note that the sum of the quantities of alkaline and alkaline earth (Na_2O, K_2O, CaO, MgO) is less than 4%. The K_2O content (0.50%) would indicate the presence of a mica phase such as illite (Kieufack *et al.*, 2023).

Table 1. Chemical composition of KOU

Oxides	SiO_2	Al_2O_3	Fe_2O_3	Na_2O	K_2O	CaO	MgO	FL*	Total
% Weight Conc.	58.55	28.38	1.66	0.08	0.50	0.01	0.21	12.32	101.71

** Fire loss*

The infrared absorption spectrum of KOU was recorded in the region from 4000 to 400 cm^{-1}. The infrared spectrum (**Figure 3**) shows the vibrations of the Al-OH bonds of kaolinite at 3695 cm^{-1} and 3620 cm^{-1} (Garcia *et al.*, 2020). The vibration at 1008.6 cm^{-1} is attributed to the O-H bond of illite but

also of kaolinite. The band around 1032 cm^{-1} was attributed to vibrations of the Si-O bond of kaolinite (Munvuyi *et al.*, 2022***)*** also of the Fe-OH bond of goethite. The presence of quartz in the sample was proven by the vibration band of the Si-O bond at 794 cm^{-1} (Munvuyi *et al.*, 2022).

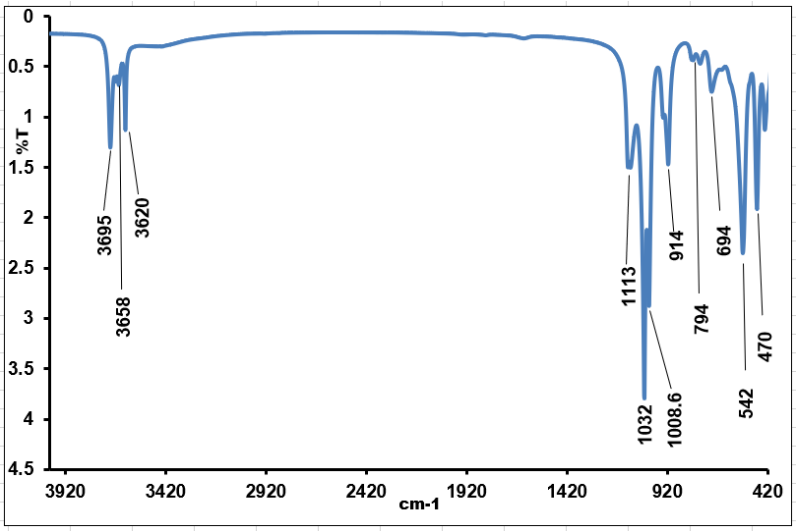

Figure 3. Infrared spectrum of the KOU

The analysis of the KOU diffractogram (**Figure 4**) shows that the main phases observed are Kaolinite, Illite, Quartz and Goethite. These results corroborate with those of chemical analysis and infrared spectrometry. The main (intense) peaks observed on the KOU diffractogram are those of kaolinite and quartz. This result suggests that KOU is mainly composed of these minerals.

The semi-quantitative analysis of the different mineral phases (**Table 2**) was carried out by coupling the results of X-ray diffraction and chemical analysis and using **Eqn.1**:

$$T(x) = \sum_1^n M_i \times P_i(x) \qquad \textbf{Eqn.1}$$

Where T(x) is the oxide percentage of chemical element x, Mi the percentage of mineral i in the sample containing chemical element x and Pi(x) the proportion of element x in mineral i (calculated from the formula of the ideal mineral).

The following chemical assignments were made:

- K_2O was attributed to illite (detected by XRD and Infrared);
- Fe_2O_3 was attributed to goethite (detected by XRD and Infrared);
- Al_2O_3 was used to calculate the contribution of kaolinite (detected by XRD and Infrared) after subtracting the contribution of illite;
- SiO_2 was used to calculate the contribution of quartz (detected by XRD and Infrared) after subtracting the contribution of kaolinite, illite.

The proportions of the different mineral phases summarized in Table 2 show that the sample is composed of kaolinite (69 %), quartz (23 %), illite (6 %) and goethite (2 %). Kaolinite is the most abundant mineral, which indicates that KOU could be considered as a kaolinitic clay due to the high proportion of Kaolinite (69 % > 50 %). It is followed by quartz and goethite are low in KOU. The mineralogical composition reflects that KOU is a raw material suitable for the synthesis of Kaolinite Nanoparticles (KNP).

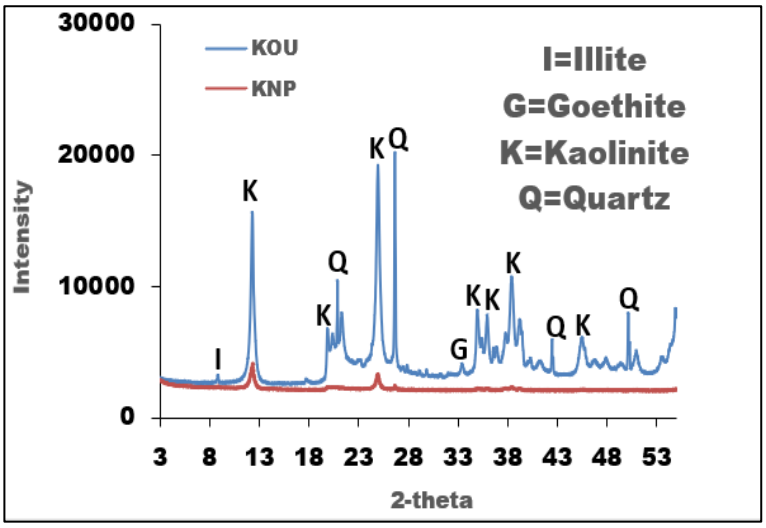

Figure 4. XRD spectra of KOU and KN

Table 2. Semi-quantitative analysis of KOU

Mineral phase	Kaolinite	Quartz	Illite	Goethite	Total
% **Weight Conc.**	69	23	6	2	100.00

3.2. *Characterization of kaolinite nanoparticles (KNP)*

The X-ray diffraction of the prepared KNP is shown in **Figure 4**. X-ray diffraction analysis showed that kaolinite $Al_2Si_2O_5(OH)_5$ is the main mineral present with other trace minerals such as Illite and quartz (SiO_2). Indeed, the peaks attributed to quartz, Illite and goethite have either drastically decreased in intensity (for quartz) or disappeared (quartz and goethite) on the diffractogram of the KNP sample. The results obtained indicate that the use of hydrochloric acid (HCl) made it possible to eliminate almost all of the associated minerals making up the KOU sample. These results agree with those expected according to the literature (Alasadi *et al.*, 2019). The X-ray diffraction method was used for the determination of the sizes of KNP. **Eqn.2** makes it possible to calculate the size distribution of KNP particles. **Figure 5** shows made it possible to determine the necessary parameters for calculating the sizes (L):

$$L = \frac{k\lambda}{\beta Cos\theta} \qquad \textbf{Eqn.2}$$

with L: particle size in nanometer (nm); λ: wavelength in angstrom (0.1540598 nm); K: constant (0.9); β: width at half height of the peak in radian (rd); Θ: theta angle in degrees.

The particle size calculated from equation **Eqn.2** is between 32 and 122 nm and the average size of KNP is 77 nm. This result would indicate that kaolinite nanoparticles were successfully produced from KOU.

4. Adsorption of chromium (VI) by KNP

4.1. Effect of contact time

The result of the kinetic experiments in **Figure 6** shows that the adsorption amount of Cr(VI) increases with contact time and stabilizes after 180 minutes. It is important to note that this increase is

not uniform. During the first 30 minutes, adsorption increases rapidly, followed by a slowdown in adsorption marked by a lower slope until the shape of the curve becomes horizontal, reflecting equilibrium. We can attribute this behaviour to the greater availability of active sites at the beginning of the adsorption process.

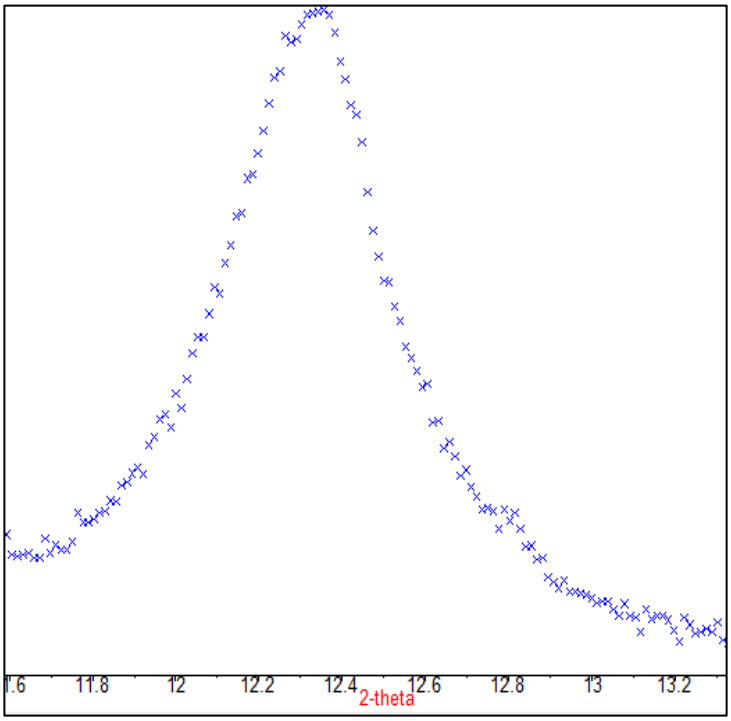

Figure 5. Zoom of one pic of the XRD of KNP

Nasanjargal *et al.*, 2021, attribute the results observed during the first 30 minutes to the processes of electrostatic interactions between the protonated surfaces of the adsorbent and the Cr(VI) ions. The stirring time of 180 minutes will be used as the time necessary to reach equilibrium for the other tests.

For the kinetic study (**Figures 7** and **8**), the mathematical equations of the pseudo-first order model (**Eqn. 3**) and the pseudo-second model (**Eqn. 4**) were used to identify the type of adsorption implemented.

Pseudo-First order model (Gallo-Cordova *et al.*, 2019)***:***

$$ln(Q_e - Q_t) = ln\, Q_e - k_1 \times t \qquad \textbf{Eqn. 3}$$

Pseudo-second order model:

$$\frac{t}{Q_t} = \frac{1}{k_2 \times Q_e^2} + \frac{t}{Q_e} \qquad \textbf{Eqn. 4}$$

where Q_t is the quantity of arsenic adsorbed at time t in mg/g, k_1 represents the pseudo-first order kinetic constant in min^{-1}, k_2 is the pseudo-second order kinetic constant in g/mg.min and Q_e represents the quantity of Cr(VI) adsorbed at equilibrium.

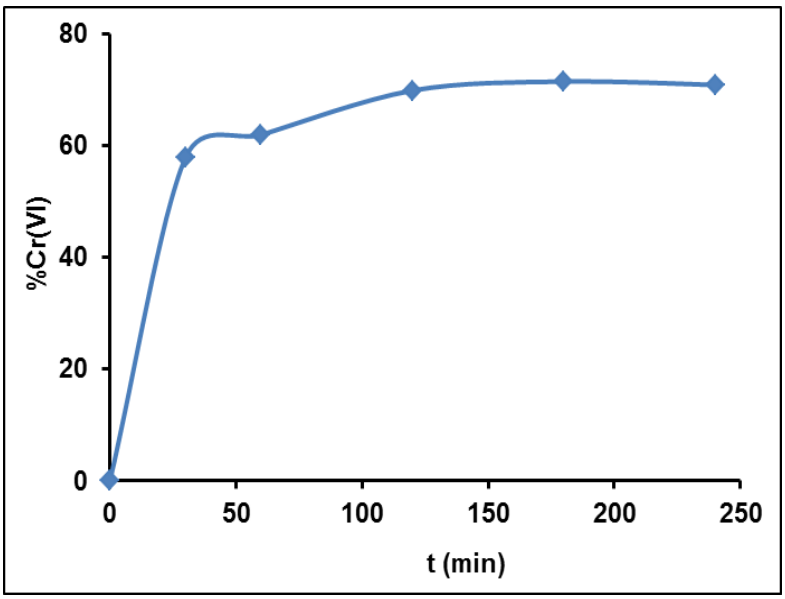

Figure 6. Effect of contact time

The coefficient of determination of the pseudo- second order kinetic model (R_2=0.9993) is slightly better than that of the pseudo-first order kinetic model (R_1=0.9325). Also, the theoretical adsorption capacity Q_e(cal) of the pseudo-second order kinetic model (Q_e=74.07 mg/g) was more similar to that measured experimentally Q_e(exp) (Q_e=75 mg/g). It is therefore likely that the pseudo-second model provides a better fit than the pseudo-first order model (Q_e=18.12 mg/g). These results show that the adsorption of Cr(VI) by KNP could occur through the formation of a high-energy chemical bond.

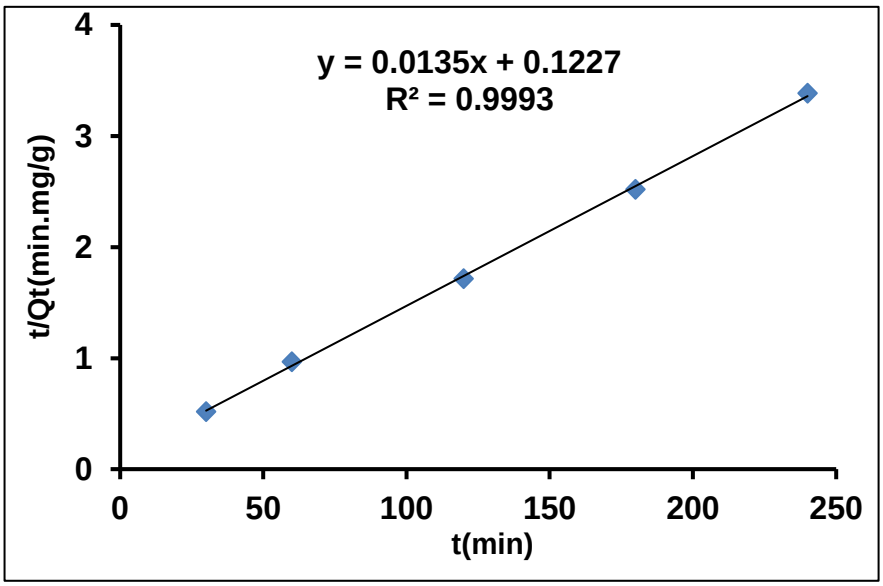

Figure 7. Pseudo-second order kinetic model

4.2. Adsorption isotherm

Figure 9 illustrates the adsorption isotherm of Cr(VI) on KNP for a concentration range of 0–0.025 g/L. The shape of the curve is similar to the type I isotherm: isotherm typical of monolayer adsorption (Mohammad *et al.*, 2020***)***. It corresponds to the filling of micropores with saturation when the layer is completely filled (Mohammad *et al.*, 2020***)***. This isotherm reflects a relatively strong interaction between the adsorbate and the adsorbent and it is entirely reversible over the entire pressure

range. The adsorption equilibrium data were correlated with both Langmuir and Freundlich models. These models express the relationship between the adsorption capacity (q_e) and the Cr(VI) concentration in the solution (C_e) at equilibrium. The Langmuir model is suitable for single-layer adsorption, assuming that the surface of the adsorbent is homogeneous, the heat of the adsorption process is constant, and there is no interaction between the adsorbed species (Ni *et al.*, 2019). This model determines the maximum adsorption capacity (Q_m) and the coefficient (b_o) related to the binding affinity, which was calculated from the slope and the intercept. The linear forms are the Langmuir model **Eq 5** and Freundlich model **Eqn. 5** (Gallo-Cordova *et al.*,2019):

$$\frac{1}{Q_e} = \frac{1}{Q_m} + \frac{1}{b_o \times Q_m} \times \frac{1}{C_e} \qquad \textbf{Eqn.5}$$

$$ln\, Q_e = ln\, k_F + \frac{ln\, C_e}{n} \qquad \textbf{Eqn.6}$$

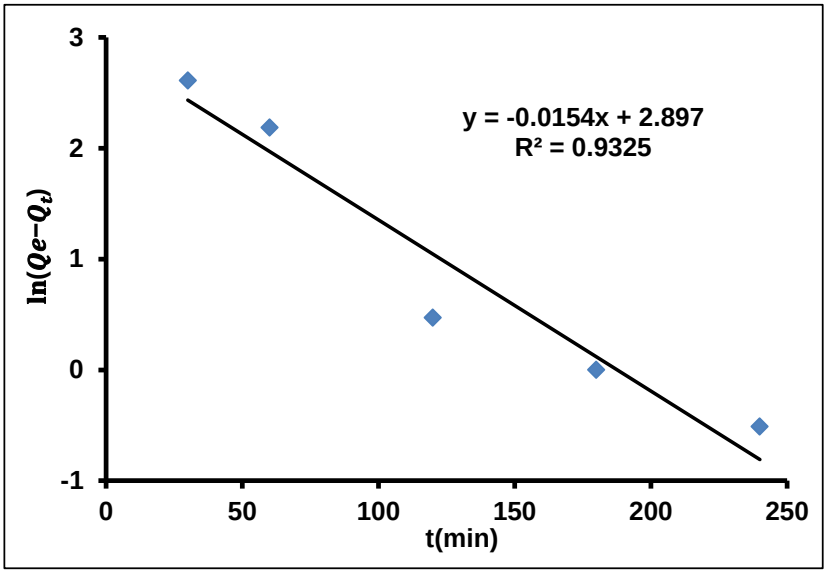

Figure 8. Pseudo-first order kinetic model

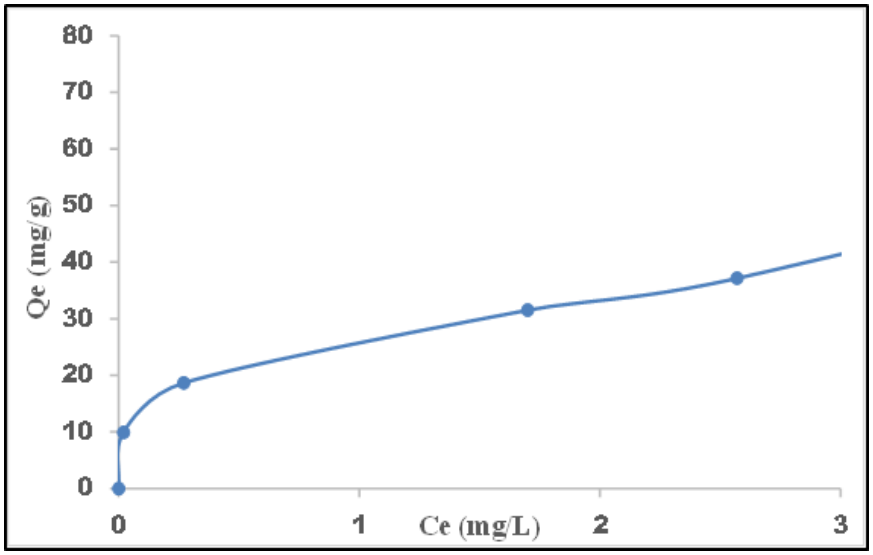

Figure 9. Adsorption isotherm

The Langmuir and Freundlich isotherms are presented respectively in **Figures 10** and **11**. The high values of the determination coefficients (R^2) of the two models suggest that the exploitation of experimental data adapts well to the Langmuir and Freundlich model. However, the coefficient of determination (R^2) of the Langmuir model (R^2=0.9901) is slightly higher than that of Freundlich (R^2=0.9678).

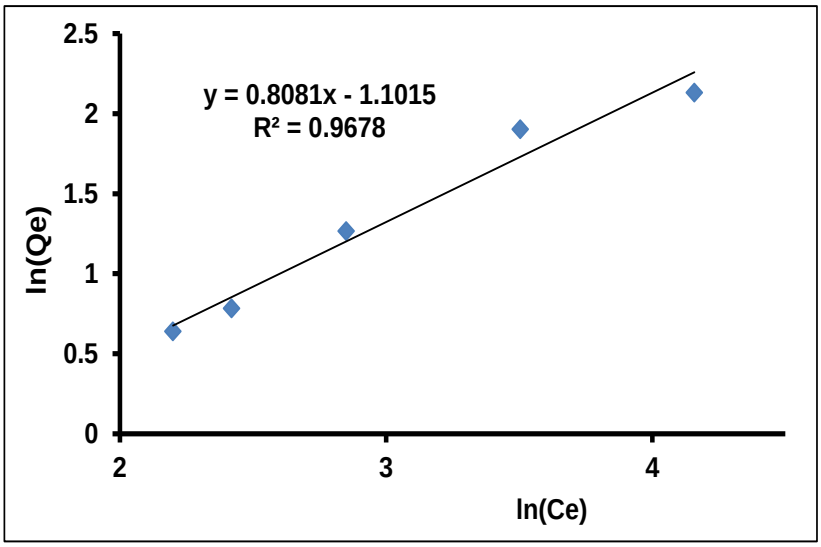

Figure 10. Freundlich model

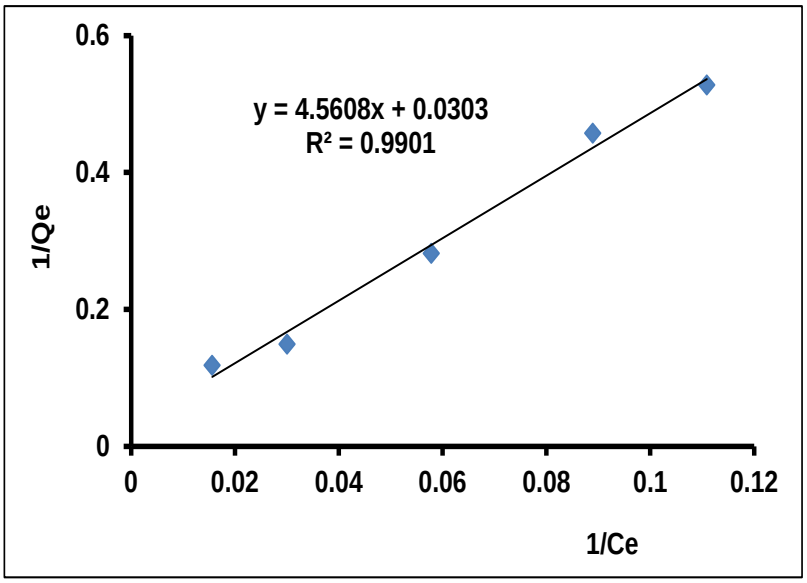

Figure 11. Langmuir model

4.3. Effect of pH

The effect of pH on the adsorption of Cr(VI) is represented by **Figure 12**. pH is a very important parameter in the Cr(VI) removal process and affects both the surface charges of the adsorbent and the types of Cr(VI) species in solution. Depending on the hexavalent concentration and pH (**Figure 13**), it exists in the chromate (CrO_4^{2-}), or the dichromate ($Cr_2O_7^{2-}$) forms. At pH <8, the chromium E-pH diagram shows the predominance of dichromate ($Cr_2O_7^{2-}$). In lower total chromium concentrations (≤ 1 g/L), $HCrO_4^-$ and CrO_4^{2-} are predominant forms, and at pH < 6, the $HCrO_4^-$ form is predominant

while at pH > 6, it is the CrO_4^{2-} form. An increase in pH leads to a decrease in the level of Cr(VI) adsorbed. **Figure 12** shows that chromium sorption fall lower than 50 % in pH ≥ 5 (greater than the zero charge pH of the adsorbent, which is 3.5). The adsorption of Cr(VI) by KNP could therefore be attributed to the electrostatic attraction between the positive surface charge of KNP at acid pH and $HCrO_4^-$ anions. In the high acidic solutions, the hydroxyl groups on the surface of KNP become protonated and therefore constitute the active sites favourable to eliminate chromate ions.

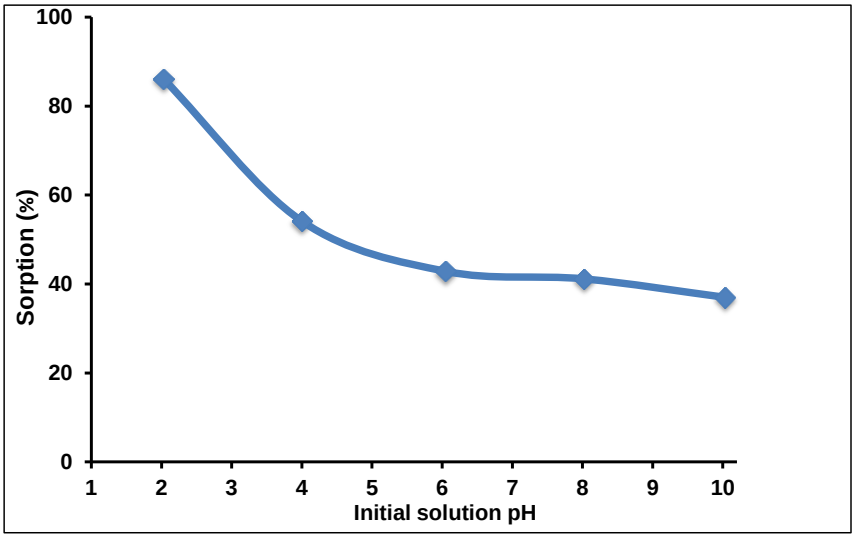

Figure 12. Effect of pH

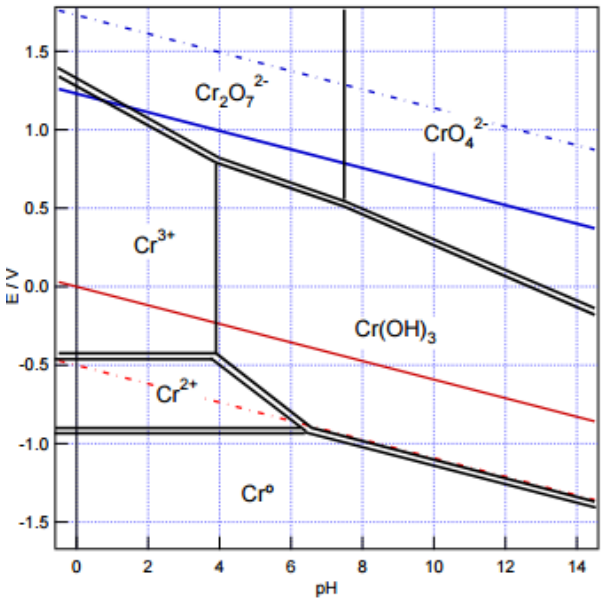

Figure 13. E-pH diagram of Chromium

4.4. KPN concentration effect

The quantity of adsorbed Cr(VI) increases with the increase in the mass of KNP (**Figure 14**). These results can be attributed to the availability of active sites on KNP. However, an increase in adsorbent slightly above 1.5 g/L does not result in a further increase in Cr(VI) absorption. It is likely that with a higher mass of KNP, there would be greater mobility of Cr(VI) due to greater accessibility of active sites replaceable by these ions.

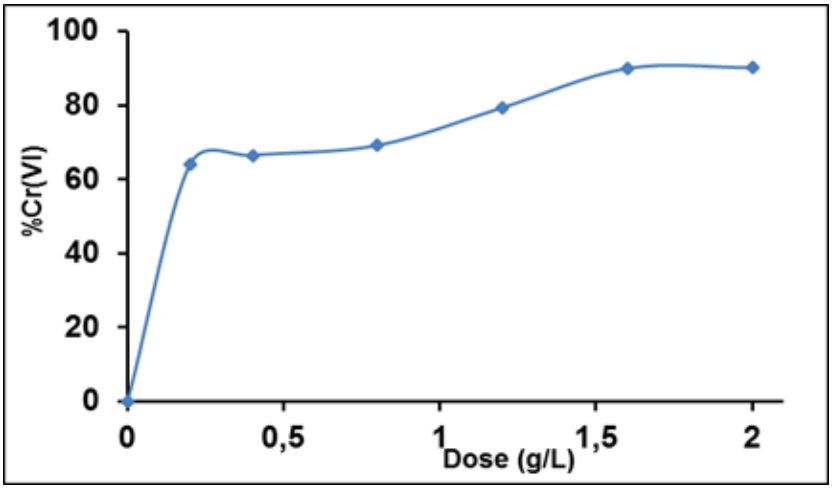

Figure 14. KNP dose effect

Conclusion

A clay called KOU was used as a raw material in the synthesis of kaolinite nanoparticles (referenced KNP). The kaolinite nanoparticles thus obtained were used as an adsorbent in the removal of Cr(VI) in synthetic water. Before any synthesis, KOU clay was characterized and the results of the characterization revealed that KOU is mainly made up of kaolinite (69 %) and other minerals such as Illite (6 %), Quartz (23%) and Goethite (2 %). In view of its high kaolinite content, KOU was classified as a kaolin clay and suitable for the synthesis of KNP. KNP were synthesized by the acid extraction process and used for the adsorption of Cr(VI) in synthetic waters. The parameters that can control the adsorption process of Cr(VI) on NPK (pH, contact time, the dose of KNP and the initial concentrations of Cr(VI)) gave appreciable results. 2 g/L of KNP adsorbs 90% of Cr(VI) in synthetic waters (20 mg/L of Cr(VI)) at pH=2 and t=180 min. Furthermore, the modelling results are in agreement with pseudo-second-order kinetics and the Langmuir isotherm. These results reflect a probable adsorption of Cr(VI) via a chemical bond to the surface of KNP (chemisorption). In the continuation of our work, we plan to explore the effects of ions competing with chromium ions during the adsorption process in order to consider its potential use in real tannery waters.

Acknowledgements, the authors are very much grateful to the International Science Programme (ISP, Uppsala, Sweden) for their financial support and IRCER from University of Limoges (France) for their technical, to carry out this research work.

Disclosure statement: *Conflict of Interest:* The authors declare that there are no conflicts of interest.
Compliance with Ethical Standards: This article does not contain any studies involving human or animal subjects.

References

Alasadi, A. M., Khaili, F. I. and Awwad, A. M., (2019) Adsorption of Cu(II), Ni(II) and Zn(II) ions by nano kaolinite: Thermodynamics and kinetics studies, *Chemistry International* 5(4) 258-268**.** https://doi.org/10.31221/osf.io/7udp2.

Azzaoui K., Mejdoubi E., Lamhamdi A., Lakrat M., Hamed O., et al. (2019) Preparation of hydroxyapatite biobased microcomposite film for selective removal of toxic dyes from wastewater, *Polymer* 1 (27), 28

Bazié B.S.R., Compaoré M.K.A., Bandé M. *et al.*, (2022) Evaluation of metallic trace elements contents in some major raw foodstuffs in Burkina Faso and health risk assessment. *Sci Rep* ***12***, 4460**.** https://doi.org/10.1038/s41598-022-08470-z.

El Harti M., Hannache H., Khouya E., Hanafi N., El Bouchti M., Zarrouk A., et al., (2013). Hexavalent chromium removal from aqueous solution by adsorbent prepared from Moroccan oil shale of Timahdit, *Der Pharmacia Lettre* 5, 338-346

Errich A., Azzaoui K., Mejdoubi E., Hammouti B., Abidi N., Akartasse N., Benidire L., EL Hajjaji S., Sabbahi R., Lamhamdi A. (2021), Toxic heavy metals removal using a hydroxyapatite and hydroxyethyl cellulose modified with a new Gum Arabic, *Indonesian Journal of Science & Technology*, 6(1), 41-64

Gallo-Cordova A., Morales M. D. P., et Mazarío E., (2019) Effect of the Surface Charge on the Adsorption Capacity of Chromium(VI) of Iron Oxide Magnetic Nanoparticles Prepared by Microwave-Assisted Synthesis, *Water*, vol. 11, n° 11, p. 2372**.** https://doi.org/10.3390/w11112372.

Garcia-Valles M., P. Alfonso, S. Martínez, N. Roca, (2020) Mineralogical and Thermal Characterization of Kaolinitic Clays from Terra Alta (Catalonia, Spain), *Minerals*, vol. 10, n° 2, p. 142**.** https://doi.org/ 10.3390/min10020142.

Kieufacka G., Fagelb N., Tchambac A.B., Bomenid I.Y., Ngapgued F., Ouahabib M. El and Wouatong A.S.L., (2023) Mineralogical and physico-chemical characterization of alluvial clays from Bamendou-Balessing (West Cameroon): Suitability for ceramics**.** *Construction and Building Materials*, 407 133396**.** https://doi.org/10.1016/j.conbuildmat.2023.133396

Kingsley Eghonghon Ukhurebor, Uyiosa Osagie Aigbe, Robert Birundu Onyancha, Wilson Nwankwo, Otolorin Adelaja Osibote, Hugues Kamdem Paumo, Onoyivwe Monday Ama, Charles Oluwaseun Adetunji, Israel Uzuazor Siloko (2021) Effect of hexavalent chromium on the environment and removal techniques: A review, *Journal of Environmental Management*, 280 111809**.** https://doi.org/10-1016/j.jenvman.2020.111809.

Mohammad A. Al-Ghouti and Dana A. Da'ana, (2020) Guidelines for the use and interpretation of adsorption isotherm models: A review**.** *Journal of Hazardous Materials*, 393 122383**.** https://doi.org/10.1016/j.jhazmat.2020.122383.

Munvuyi D., Ousmane M. S. and Bougouma M., (2022) Physicochemical and mineralogical characterization of clays from the Tcheriba zone in the Boucle of Mouhoun region (Burkina Faso). *J. Mater. Environ. Sci.*, Volume 13, Issue 07, Page 755-767. http://www.jmaterenvironsci.com

Nasanjargal S., Munkhpurev B. A., Kano K., Kim H. J**.** and Yunden Ganchimeg**,** Y., (2021) The Removal of Chromium (VI) from Aqueous Solution by Amine-Functionalized Zeolite: Kinetics, Thermodynamics, and Equilibrium Study**.** *Journal of Environmental Protection*, 12, 654-675**.**
https://doi.org/10.4236/jep.2021.129040

Ni B. J., Huang Q. S**.**, Wang C., Ni T. Y**.**, Sun J. and Wei W., (2019) Competitive adsorption of heavy metals in aqueous solution onto biochar derived from anaerobically digested sludge**.** *Chemosphere*, 219 351e357**.** https://doi.org/10.1016/j.chemosphere.2018.12.053

Njugunaa S. M., Makokhaa V. A., Yana X., Giturud R. W., Wanga Q. and Wang J., (2019) Health

risk assessment by consumption of vegetables irrigated with reclaimed waste water: A case study in Thika (Kenya). *Journal of Environmental Management,* 231 576-581**.** https://doi.org/10.1016/j.jenvman.2018.10.088.

Pakade V. E., Tavengwa N. T., and Madikizela L. M., (2019) Recent advances in hexavalent chromium removal from aqueous solutions by adsorptive methods. *RSC Advances,* 9(45), 26142–26164**.** https://doi.org/10.1039/C9RA05188K.

Razzouki B., El Hajjaji S., Azzaoui K., A Errich, A Lamhamdi, et al.; (2015). Physicochemical study of arsenic removal using iron hydroxide, *J. Mater. Environ. Sci.* 6 (5), 144-1450

Shiv Prasad, Krishna Kumar Yadav, Sandeep Kumar, Neha Gupta, Marina M.S. Cabral-Pinto, Shahabaldin Rezania, Neyara Radwan, Javed Alam, (2021) Chromium contamination and effect on environmental health and its remediation: A sustainable approaches. *Journal of Environmental Management,* 285 112174**.** https://doi.org/10.1016/j.jenvman.2021.112174

Sawadogo W.A.M., Zoungrana T. D. (2024), Environmental effects of waste electrical and electronic equipment valorization in burkina faso, Environmental Advances, Volume 17, 2024, 100559, ISSN 2666-7657, https://doi.org/10.1016/j.envadv.2024.100559

Tariq F.S., (2021) Heavy metals concentration in vegetables irrigated with municipal wastewater and their human daily intake in Erbil city. *Environmental Nanotechnology, Monitoring & Management,* 16 100475**.** https://doi.org/10.1016/j.enmm.2021.100475.

Vardhana K. H., Kumara P. S. and Panda R. C. A, (2019) Review on heavy metal pollution, toxicity and remedial measures: Current trends and future perspectives. *Journal of Molecular Liquids,* 290 111197**.** https://doi.org/10.1016/j.molliq.2019.111197